

## HYBRID ALGORITHM BASED PARALLEL SOLUTION TO ELECTROMAGNETIC SCATTERING FOR ARBITRARY SHAPED CAVITIES

XIAO-LI ZHI, WEI-QIN TONG, YUE HU, PENG CHEN, AND JUN-GAO HU

**Abstract.** The Radar Cross Section (RCS) prediction for cavities is significant to measure a target's radar detection ability. For electrically large, deep, arbitrary shaped cavities, this paper presents a hybrid algorithm based parallel solution using Message Passing Interface on distributed memory computers. The meaning of 'Hybrid' here is threefold. First, the RCS for cavities is modeled and calculated with a hybrid algorithm of IPO (Iterative Physical Optics), FMM (Fast Multipole Method) and Generalized Reciprocity Integral (GRI) combined by a cascading segmentation technique. Second, a hybrid approach is applied to the two phases of parallelization. On phase of geometrical preprocessing, all parallel processes assume a whole workload to construct the cavity geometry independently. On the other phase of electromagnetic computing, the workload is distributed by domain decomposition. Third, the decomposition scheme is hybrid as facets are decomposed to compute near-field interaction while angle samples are used to distribute far-field interaction. The superposition of electromagnetic measures and permutability of math vector operations are fully exploited to do partial computation in order to minimize the communication overhead. The hybrid parallel solution can achieve very good tradeoff between memory and time. It yields a good load balance while still keeping the parallel code pretty concise. Numerical results show near-linear scalability and over 90% parallel efficiency.

**Key words.** Radar Cross Section, Cavity, Parallel, Iterative Physical Optics, Fast Multipole Method, Hybrid algorithm.

### 1. Introduction

As a measure of the detection ability of a target in radar systems, the Radar Cross Section (RCS) has been an important topic in electromagnetic research. The RCS prediction for cavities is particularly important for its dominance in the target's entire RCS. For example, the engine inlet and exhaust ducts may contribute very significantly to the RCS of modern jet aircraft. Thanks to its significant industrial and military applications, the cavity problem has attracted much attention. A variety of methods, such as Waveguide Model Analysis, IPO (Iterative Physical Optics) and FMM (Fast Multipole Method), have been proposed to solve the arbitrary shaped cavity problems [1][2][3][4]. For arbitrary shaped and electrically large cavities, a hybrid algorithm connecting IPO, FMM and GRI (Generally Reciprocal Integral) with Cascading Segmentation scheme was recognized to be an efficient way to solve scattering problems. A serial implementation of the hybrid algorithm was presented by our partners [5]. Tested experiments demonstrated its accuracy and efficiency in comparison with model reference solutions.

However, when the number of unknowns becomes very large, say tens or hundreds of thousands, it is beyond the capability of the serial version with respect

---

Received by the editors March 1, 2010 and, in revised form, December 12, 2010.

2000 *Mathematics Subject Classification.* 35R35, 49J40, 60G40.

This work is supported in part by Shanghai Leading Academic Discipline Project, Project Number:J50103, and by Aviation Industry Development Research Center of China. Experiments were done by the support of High Performance Computing Center at Shanghai University which provides computing infrastructure of ZiQiang3000 cluster for this work.

to memory requirement or time requirement. Although FMM and its recursive variant, the multilevel fast multipole algorithm (MLFMA), have been successfully implemented on various parallel computers and their good performance has been well reported [6][7][8][9][14], it is not so in the case of the hybrid algorithm for cavities. Indeed, there have been very few attempts at parallel implementation for analysis of RCS of cavities. In [13] a parallelization approach of the finite element-boundary integral-multilevel fast multipole algorithm (FE-BI-MLFMA) is presented for scattering by large and deep coated cavities loaded with obstacles. And [11][12] introduces our preliminary work on parallelizing IPO and FMM for straight cavities. This paper will extend the range of problems that can be solved by the previous serial implementation and discuss the parallelization based on the hybrid algorithm to compute RCS of any electrically large, deep and arbitrarily shaped cavities using the Message Passing Interface (MPI) [15].

The rest of this paper is organized as follows. In Section 2 the primary computation of the serial hybrid algorithm is briefly reviewed, which provides a basis for parallelization. In Section 3, the parallel methodology is discussed, followed by a detailed analysis of communication, computation and storage overhead. Numerical results are presented in Section 4 to demonstrate the effectiveness of the parallel solution. Finally comes the summary.

## 2. Hybrid algorithm for RCS of cavities

To analyze the highly complex high-frequency scattering problem from electrically large open cavities, IPO approach [1] was proposed by F.O.Basteiro etc. in 1995 which iteratively applies the high-frequency asymptotic principles of physical optics to account for multiple reflections inside the cavity. The IPO algorithm has been shown as a much efficient and high accurate although numerically intensive approach in analyzing electro-magnetic scattering by very large and complex cavities. The FMM, an approximation technique which reduces the complexity of matrix vector product of  $M$  order from  $O(M^2)$  to  $O(M^{1.5})$ , was proposed by Rokhlin at the University of Yale in the end of 80s. It was applied by C.C. Lu, etc. to accelerate the RCS computing of large and complex objects [7]. And FMM could also be employed to speed up the iterative process of IPO [5]. The Segmented approach for analyzing the electromagnetic scattering of arbitrary shaped cavities [3] was also proposed by F. O. Basteiro etc in 1998. In this approach, the cavity is divided into two different parts: the front section (typically smooth) and the complex termination. The front section is subdivided into several sections, see Figure 1 for an illustration, where  $W^+ = \begin{bmatrix} E^+ \\ H^+ \end{bmatrix}$ ,  $W^- = \begin{bmatrix} E^- \\ H^- \end{bmatrix}$  are the tangential components of the incident and reflective electromagnetic field respectively. Each section is analyzed independently from the rest of the cavity. Generalized Reciprocity Integral (GRI), proposed by Pathak and Burkholder in 1993 [4] for cavity with complex termination, is applied to the segmented approach to avoid retracing back, which is quite time-consuming.

For the RCS problem of arbitrary shaped and electrically large cavities with complex termination, a hybrid algorithm combined IPO, FMM and GRI with Cascading Segmentation technique is more desirable for accuracy and efficiency than any single method of them [5]. The computation process for the hybrid algorithm is briefly described as follows.

**Step1—Incident Field on Wall (IFW):** For section  $k$ , the incident magnetic field on the inner wall induced by electromagnetic fields (or incident wave when

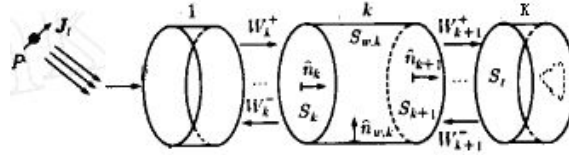


FIGURE 1. Cavity model with K sections split.

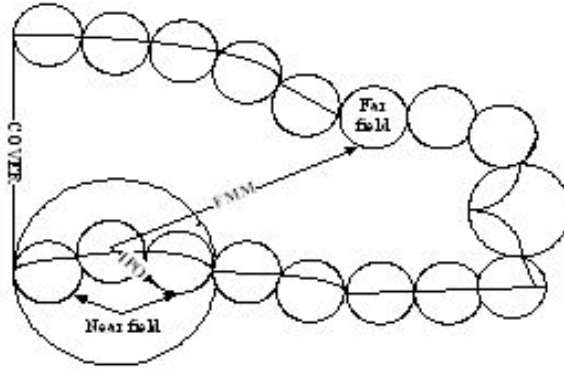


FIGURE 2. Domain decomposition of cavity facets.

$k = 1$ ) on the section's cover is obtained using Kirchhoff approximation, formulated as (1).

$$(1) \quad H_k^{inc}(r) = \int_{S_k} \hat{n}_k \times H_k^+(r') \times \nabla G_0(r - \hat{r}) ds' + \frac{1}{jkZ_0} \nabla \times \int_{S_k} E_k^+(r') \times \hat{n}_k \times \nabla G_0(r - \hat{r}) ds'$$

**Step2—Stable Current on Wall (SCW):** For section  $k$ , an iterative solution is applied to the magnetic field integral equation until the stable current on the inner wall is reached using multiple reflections inside the cavity, refer to (2) where  $i$  is the iteration counter.

$$(2) \quad J_{w,k}^i(r) = 2\hat{n}_{w,k} \times H_k^{inc}(r) + 2\hat{n}_{w,k} \times \int_{S_{w,k}} J_{w,k}^{i-1}(r') \times \nabla G_0(r - \hat{r}) ds'$$

**Step3—Incident field on Next Cover (INC):** For section  $k$ , the total electromagnetic fields on section  $k + 1$  cover, induced by the stable current from the inner wall of section  $k$  and the electromagnetic fields from the cover of section  $k$ , are calculated, using a simplified connection scheme based on Kirchhoff approximation, see (3). Then, go to step 1 until  $k < K$ .

(3)

$$\begin{aligned}
H_{k+1}^+(r) &= \hat{n}_{k+1} \times \left( \int_{S_{w,k}} J_{w,k}(r') \times \nabla G_0(r - \hat{r}) ds' + \int_{S_k} \hat{n}_k \times H_k^+(r') \times \right. \\
&\quad \left. \nabla G_0(r - \hat{r}) ds' + \frac{1}{jkZ_0} \nabla \times \int_{S_k} E_k^+(r') \times \hat{n}_k \times \nabla G_0(r - \hat{r}) ds' \right) \times \hat{n}_{k+1} \\
E_{k+1}^+(r) &= \hat{n}_{k+1} \times \left( \frac{Z_0}{jk} \nabla \times \int_{S_{w,k}} J_{w,k}(r') \times \nabla G_0(r - \hat{r}) ds' + \frac{Z_0}{jk} \nabla \times \int_{S_k} \hat{n}_k \times \right. \\
&\quad \left. H_k^+(r') \times \nabla G_0(r - \hat{r}) ds' - \int_{S_k} E_k^+(r') \times \hat{n}_k \times \nabla G_0(r - \hat{r}) ds' \right) \times \hat{n}_{k+1}
\end{aligned}$$

**Step4—Reflective field on Last Cover (RLC):** For the last section ( $k = K$ ), the reflective electromagnetic fields on its cover induced by the stable current from its inner wall are calculated again using Kirchhoof approximation.

$$\begin{aligned}
(4) \quad H_K^-(r) &= \int_{S_{w,K}} J_{w,K}(r') \times \nabla G_0(r - \hat{r}) ds' \\
E_K^-(r) &= \frac{Z_0}{jk} \nabla \times \int_{S_{w,K}} J_{w,K}(r') \times \nabla G_0(r - \hat{r}) ds'
\end{aligned}$$

**Step5—RCS:** The GRI is used to obtain the global response of the whole cavity at the termination, refer to (5).

$$(5) \quad \hat{p} \cdot E_P^s(P) \approx \int_{S_K} (E_K^- \times H_K^+ - E_K^+ \times H_K^-) \cdot \hat{n}_K ds$$

The Step3 involves interaction of currents between facets, which is the real combination of IPO and FMM and actually a large scale linear equation system of three-dimensional complex vector elements. It contributes most to the total computation. The basic principle behind FMM here is to decompose the interaction, thus the computation of matrix vector product, into two parts: near-field interaction between nearby sources and far-field interaction between well separated ones. To get such decomposition, the sources are enclosed in many group boxes with the same size (see Figure 2 for an illustration). Sources from two groups are neighbors only if the distance between their belonged boxes is in certain range. The near-field interaction is directly calculated using IPO method while far-field interaction is more divided into three stages called the aggregation phase, the translation phase and the disaggregation phase [8]. Equation (2) can be re-formulated as (6), where  $V_f, \alpha, V_s$  are called aggregation factor, translation factor and disaggregation factor for the three stage. The factors can be calculated before the iteration for they don't change with the currents and incident wave.

$$\begin{aligned}
(6) \quad H_{far} &= \int d^2 \hat{k} V_{fm,j}(\hat{k}) \sum_{m' \in Far} \alpha_{mm'}(\hat{k} \cdot r_{mm'}) \sum_{i \in m'} V_{sm'i}(\hat{k}) J_{w,k}^{i-1}(r') \\
H_{near} &= \sum_{m \in Near} \int_{S_{w,k,m}} J_{w,k}^{i-1}(r') \times \nabla G_0(r - \hat{r}) ds' \\
J_{w,k}^i &= 2\hat{n}_{w,k} \times H_k^{inc} + 2\hat{n}_{w,k} \times (H_{near} + H_{far})
\end{aligned}$$

### 3. Hybrid approach for parallelization

The computation process described above is serial in nature. The next step will operate on data prepared by its previous steps. For such problem, the principle of parallelization is to decompose data domain properly and evenly so that partial computation in each step can be done on partial data as independently as possible. Thus keeping the integrity of data structures and their correlation is the key problem for parallelization.

The computer implementation of the hybrid algorithm models the cavity with roughly triangular flat facets. The electric and magnetic fields are assumed constant on one facet. The integral on unit sphere  $\int d^2\hat{k}$  is calculated as the numerical integral on  $2L^2$  angle samples ( $L$  is called mode number, depending on the size of maximum group). The discrete version of above formulae is given in Table 1. To avoid overburden of mathematic symbols, a general 'f' is used to stand for the electromagnetic relation and 'T' for geometrical or topological data, while  $x, y, \hat{k}$  denotes a member of wall facets  $S_{w,k}$ , cover facets  $S_k$  or angle samples  $S_a$ .

**3.1. Full replication of geometric topology.** From Table 1, it can be recognized that geometric data is heavily involved in single calculation of every step. Either all cover facets are required or all wall facets are called for. The layout of geometric structures in parallel processes will decide the design of parallel algorithm and its efficiency.

In the case of RCS computing, there exist two important geometrical properties which influence the choice of storage model of geometric data. The first property, arising from the discretization of integral equations, is that they are stationary in time. That is, the geometry does not change with time. This property can be used to generate a good load balancing strategy during the initialization time itself.

However, the second property is not so helpful. It refers to the fact that most discretization procedures use basis functions with non-trivial support [16]. Such discretisations make the so called "connection matrix" non-diagonal. The connection matrix relates the basis functions to geometric description of the object. Therefore, any decomposition of basis functions across multiple processes will have to ensure completeness of local data. That is, one need to make sure that if a particular basis function is assigned to a processor, all the geometric data associated with that basis function is also available at the same processor. Note that a locally complete decomposition may still have replication to some extent.

One way to handle this problem is to simply replicate the full geometric structures in every process. Memory for geometric data structures is  $O(N)$ , where  $N$  is the number of unknowns and a full replication has the undesirable scaling of  $O(NP)$  where  $P$  is the total number of processes. But for cavity problems, generally ranging from hundreds unknowns to a few hundreds of thousands, this approach is very practical. For example, the memory requirement for geometric data reaches to 300MB for a case of 300 thousands of unknowns in our implementation. It is even possible to put all geometric data in the memory of a common desktop computer.

**3.2. Parallelizing electromagnetic computing.** From Table 1, another two important features can be identified. Firstly, single calculation in each step is independently from another. Secondly, each step can be formulated as the summation of certain three dimensional complex vectors on certain facet or angle sample. Thus, the computing process is proper for parallelizing based on the decomposition

of facets (noted as FDP, short for Facet Distribution Paradigm) or angle samples (noted as ADP, short for Angle sample Distribution Paradigm). ADP applies to the far-field interaction and FDP mostly relates to the near-field contribution. The distribution patterns of the hybrid parallel algorithm by steps is given in Table 2, where the superscript of  $p$  denotes a subset or a partial value, a capital  $P$  denotes the degree of parallel (in other words, the number of processes),  $F$  represents the complex expressions same as that in Table 1,  $N_w$  and  $N_k$  stands for the maximum order of all possible  $S_{w,k}$  and  $S_k$  respectively.

### FDP

In real applications, the number of facets on wall is much larger than that on cover, so wall facets  $S_{w,k}$  are chosen as the primary decomposition domain and cover facets  $S_k$  as the second if necessary.

Distributing evenly the facets is to segment the total facets into sections of same size among processes. This can be achieved by some trivial math calculations, such as the following C++ code implemented in our software:

```

quotient = facet_number / mpi_comm_size;
remainder = facet_number % mpi_comm_size;
(my_mpi_rank < remainder )? my_number = quotient + 1:
                               my_number = quotient ;
(my_mpi_rank < remainder )? my_offset = my_mpi_rank * quotient + my_mpi_rank:
                               my_offset = my_mpi_rank * quotient + remainder;

```

TABLE 1. Discretized version of the serial hybrid algorithm

Step	Discretized computation	Required data
1 : IFW	$H_k^{inc}(x) = \sum_{y \in S_k} f(H_k^+(y), E_k^+(y))$	$\forall y \in S_k, E_k^+(y), H_k^+(y)$ $\forall y \in S_k, T(y)$ $\forall x \in S_{w,k}, T(x)$
2 : SCW	$J_{w,k}^i(x) = J_{near}(x) + J_{far}(x)$ $J_{near}(x) = f(H_k^{inc}(x))$ $\quad + \sum_{x' \in N_{near}} f(J_{w,k}^{i-1}(x'))$ $J_{far}(x) = \sum_{\hat{k} \in S_\alpha} \sum_{x' \in F_{far}} f(J_{w,k}^{i-1}(x'))$ $\quad \alpha, V_s, V_f$	$\forall x \in S_{w,k}, J_{w,k}^{i-1}(x)$ $\forall x \in S_{w,k}, T(x)$ $\forall \hat{k} \in S_\alpha, \alpha, V_s, V_f$
3 : INC	$H_{k+1}^+(y) = \sum_{x \in S_{w,k}} f(J_{w,k}(x))$ $\quad + \sum_{y' \in S_k} f(H_k^+(y'), E_k^+(y'))$ $E_{k+1}^+(y) = \sum_{x \in S_{w,k}} f(J_{w,k}(x))$ $\quad + \sum_{y' \in S_k} f(H_k^+(y'), E_k^+(y'))$	$\forall y' \in S_k, E_k^+(y'), H_k^+(y')$ $\forall x \in S_{w,k}, J_{w,k}(x)$ $\forall y' \in S_k, T(y')$ $\forall x \in S_{w,k}, T(x), y \in S_{k+1}, T(y)$
4 : RLC	$H_K^-(y) = \sum_{x \in S_{w,K}} f(J_{w,K}(x))$ $E_K^-(y) = \sum_{x \in S_{w,K}} f(J_{w,K}(x))$	$\forall x \in S_{w,K}, J_{w,K}(x)$ $\forall x \in S_{w,K}, T(x), y \in S_K, T(y)$
5 : RCS	$rcs = \sum_{y \in S_K} f(E_K^-(y), E_K^+(y), H_K^-(y),$ $\quad H_K^+(y))$	$\forall y \in S_K, E_K^+(y), H_K^+(y), E_K^-(y),$ $\quad H_K^-(y)$ $\forall y \in S_K, T(y)$

Another alternate is to distribute evenly the facet groups. This will speed up the loop in computing of near-field interaction but may result load imbalance for steps related to FDP as a result of the size dis-uniformity in groups.

**ADP**

Splitting the far-field interaction computing by facets groups fails in that too complex communication would be induced by the correlativity between groups. Fortunately, the far-field interaction can be transformed as the summation on  $2L^2$  angle samples and computing on one sample is independent of another. Simply splitting the angle samples into processes is invalidated by the symmetry property

TABLE 2. Distribution pattern of the hybrid parallel algorithm

Step	Each process	
	Computation	Memory
Geo	Whole geometric processing	Full geometric data
Pre	Preprocessing : $V_f(\forall \hat{k} \in S_a^p), \alpha(\forall \hat{k} \in S_a^p)$ $V_s(\forall \hat{k} \in S_a^p)$	$V_f(\forall \hat{k} \in S_a^p), \alpha(\forall \hat{k} \in S_a^p)$ $V_s(\forall \hat{k} \in S_a^p)$
1 : IFW	$H_k^{inc}(\forall x \in S_{w,k}^p)$	$H_k^{inc}(\forall x \in S_{w,k}^p)$
2 : SCW	$J_{near}(\forall x \in S_{w,k}^p)$ $J_{far}(\forall x \in S_{w,k}) = \sum_{\hat{k} \in S_a^p} F$ $J_{w,k}^i(\forall x \in S_{w,k}^p) = J_{near}(x) +$ $J_{far}(x, \forall \hat{k} \in S_a)$	$J_{near}(\forall x \in S_{w,k}^p)$ $J_{far}(\forall x \in S_{w,k}, \forall \hat{k} \in S_a^p)$ $J_{w,k}^i(\forall x \in S_{w,k})$
3 : INC	$H_{k+1}^+(\forall y \in S_{k+1})^p = \sum_{x \in S_{w,k}^p} F + \sum_{y' \in S_k^p} F$ $E_{k+1}^+(\forall y \in S_{k+1})^p = \sum_{x \in S_{w,k}^p} F + \sum_{y' \in S_k^p} F$	$E_{k+1}^+(\forall y \in S_{k+1})$ $H_{k+1}^+(\forall y \in S_{k+1})$
4 : RLC	$H_K^-(\forall y \in S_{w,K}^p) = \sum_{x \in S_{w,K}^p} F$ $E_K^-(y)^p = \sum_{x \in S_{w,K}^p} F$	$E_K^-(\forall y \in S_K)$ $H_K^-(\forall y \in S_K)$
5 : RCS	$r_{cs} = \sum_{y \in S_K} F$	$r_{cs}$

TABLE 3. Communication overhead for the hybrid parallel algorithm

Step	Communication	Paradigm
Geo	/	/
Pre	/	ADP
1 : IFW	/	FDP
2 : SCW	/	FDP
	/	ADP
	One MPI_AlltoAll and One MPI_Allgather for each iteration	FDP
3 : INC	One MPI_Allreduce when $k < K - 1$	FDP
4 : RLC	/	FDP
5 : RCS	One MPI_Reduce	/

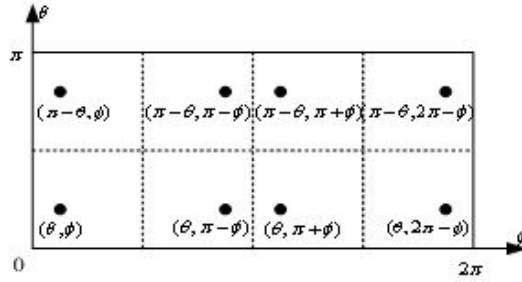


FIGURE 3. Symmetry of angle samples.

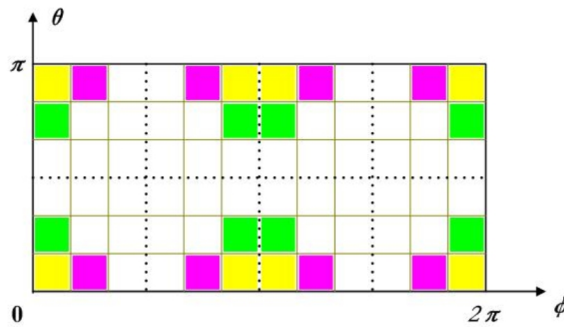


FIGURE 4. Similar angle regions assigned to the same process.

associated with translation factors [17]. This symmetry will reduce the computing and storage of the large and complex translation factor matrix up to one eighth, which can lead to quite significant savings. Other seven eighth translation factors would be obtained on the fly by mapping to their counterparts through symmetry. Studying the formula of translation factor, 8 samples coming from 8 regions are revealed to be related to the symmetry, refer to Figure 3.

The decomposition of angle samples has to assign the eight symmetric participants to the same process. One straight way is to first allocate one region (noted as seed region) of the angle sample domain, say  $\{\theta = [0, \pi/2), \phi = [0, \pi/2)\}$ , into each process then to allocate corresponding symmetric parts in the other seven regions into the same process as their seed, as demonstrated in Figure 4. One note remarkable is that the integral sampling  $[0, \dots, 2L - 1)$  with increment of  $\pi/L$  on  $\phi$  may lead to its symmetry mapping being across the region boundary. So sampling on  $\phi$  will shift to fractional values such as  $[0.5, \dots, 2L - 0.5)$ . The relative difference of RCS with fractional sampling is less than 0.01% RCS with integral sampling in experimental results.

**3.3. Analysis of the parallel algorithm.** Any parallel algorithm needs a model of communication, a model of computation, and a model of storage. Below an approximate measure to the three aspects for the parallel algorithm proposed is given.

**Computation**

Suppose FDP and ADP distribute evenly computations on facets and angle samples. The computation time for serial version can be formulated approximately as

follows:

$$(7) \quad T_1 = T_{geo} + T_{pre} + N_{iwa} (K(T_1 + N_i T_2 + T_3) + T_4 + T_5)$$

where  $N_{iwa}$  is the number of incident wave angles for which RCS need to be computed, and  $N_i$  is the iteration number to obtain stable current on wall. The hybrid parallel algorithm induces no computation overhead besides that directly concerning communication. The computation time with  $P$  parallel degree may be approximated as:

$$(8) \quad T_p = T_{geo} + \frac{T_{pre}}{P} + N_{iwa} \left( K \left( \frac{T_1}{P} + N_i \left( \frac{T_2}{P} + T_{c2} \right) + \frac{T_3}{P} + T_{c3} \right) + \frac{T_4}{P} + T_5 + T_{c5} \right)$$

The parallel efficiency is:

$$(9) \quad E_p = \frac{T_1}{T_p P} = \frac{t_s + t_p}{(t_s + t_p/P + t_c)P} \approx \frac{1}{1 + (t_c/t_p)P}$$

where  $t_s$  is the time for the serial part,  $t_p$  for the parallelized part and  $t_c$  for communication.

The time complexity for each step can be roughly measured as the number of float operations parameterized with some physical conditions. In our implementation,  $T_{geo}, T_5, T_4$  are evaluated to be the relatively small ones. Experimental results also show that  $T_{geo}$  and  $T_5$  hold really small ratio in all 'T's (less than 0.05%, refer to next section). It's reasonable to ignore the  $t_s$ . When the number of incident angles to be analyzed and the number of unknowns get larger, the  $T_{pre}, T_4, T_{c5}$  would become insignificant, thus:

$$(10) \quad \frac{t_c}{t_p} \approx \frac{N_{iwa} (K(N_i T_{c2} + T_{c3}) + T_{c5})}{T_{pre}/P + N_{iwa} (K(T_1/P + N_i T_2/P + T_3/P) + T_4/P)} > \frac{N_i T_{c2} + T_{c3}}{N_i T_2/P + T_3/P}$$

For the pretty large scale problems, the parallel efficiency can be approximated as:

$$(11) \quad E_p \approx \frac{1}{1 + T_{c2}/T_2}$$

It is obvious that the performance of MPI collective communication MPI\_Alltoall and MPI\_Allgather is determining to the parallel efficiency. In practice, it's not uncommon to yield a parallel efficiency over 95%.

Above analysis is on the presumption of the perfect distribution by FDP and ADP. In current implementation, FDP works well but ADP allocates workload not always equably. More discussions on ADP will present on next section.

### Memory

The memory consumption comprises memory for geometric data  $M_g$  and memory for electromagnetic data  $M_e$ . Let  $N_{wgt}, N_{wkt}, N_{kt}, N_{SN}, N_{Sa}$  be the number of all wall facet groups, all wall facets, all cover facets, cover facets in the last section, and angle samples respectively. For the serial implementation they can be estimated as:

$$M_g = O(40N_{wgt} + 134(N_{wkt} + N_{kt}))$$

$$M_e = M_{es} + M_{ea}$$

where  $M_{es} = O(18N_{wkt} + 12N_{wt} + 12N_{SN})$ ,  $M_{ea} = N_{sa}(66 + 20N_{wg} + 2N_{wkt})$ . So the total memory requirement locates at:

$$M_1 = M_g + M_e$$

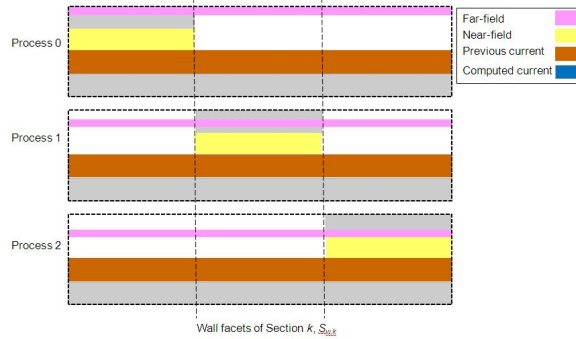


FIGURE 5. Data distributing over processes before communication.

The memory requirement on each parallel process is about:

$$M_p = M_g + M_{es} + M_{ea}/P + M_c$$

A measure named as distribution efficiency  $D_p$  is defined to evaluate the distributing effect on memory just as the parallel efficiency on computing time.

$$(12) \quad D_p = \frac{M_1}{M_p P}$$

It can be seen that the parallel algorithm proposed distributes only that portion of memory associated with angle samples over processes. The distribution efficiency falls over a relatively wide range depending on the number of facets, angle samples and processes. In our experiments, it can range from 50%~97%, finding more in next section.

### Communication

There have only communication operations in step 2, 3 and 5 as indicated in Table 3 .The communication involved in step 3 and 5 is simple but that in step 2 is somewhat sophisticated.

With the distribution paradigm of FDP, each process is responsible for calculating the incurred currents on some part of the wall facets at each iteration in step 2. For this pur-pose, each process has to collect the integrate far-field interaction, the near-field interaction and the previous iterative currents for that part of facets. Before any communication, the related data spreads out over processes as illustrated in Figure 5 ,where the absent data from one process is denoted by the gray region.

After communication and calculation, the distribution of related data should reach to such a view as showed in Figure 6.

Communication is required on two occasions:

- 1) Each process needs the remainder of the far-field interaction for its assigned fa-cets from other processes. To this end, one way is to initiate one MPI.Reduce operation for each process. Another possible way is to start one MPI.AlltoAll operation for all processes. The latter way can cut down much communication initiation time, and thus is adopted by the parallel system.
- 2) Each process needs the currents for all the facets. This can be reached simply by one MPI.Allgather operation for all processes.

The communication operations all involve MPI collective communication. Let  $T_{c2}$ ,  $T_{c3}$ ,  $T_{c5}$  be the communication time in step 2 (for one iteration step), 3 and 5 respectively. In our implementation, the time for buffer preparing, data packing and unpacking is negligible because communication buffers are allocated in advance

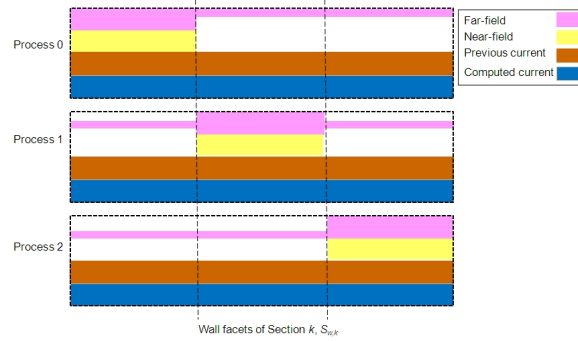


FIGURE 6. Data distributing over processes by end of iteration.

and data (un-)packing is simple.  $T_{c2}$  is equal to the time for one MPI\_Alltoall with  $N_w$  data elements plus one MPI\_Allgather with  $N_w/P$  data elements.  $T_{c3}$  accounts for one MPI\_Allreduce with  $2N_k$  data elements by MPI\_SUM operation.  $T_{c5}$  just consists of one MPI\_Reduce with one data element by MPI\_SUM operation.

The finishing time for a MPI collective communication is quite difficult to be estimated exactly. The specific send-receive algorithm used, network bandwidth and hardware infra-structure all exert their influence. The communication time for MPI\_Alltoall or MPI\_Allgather increases nearly linear with number of data elements and remarkably with the number of processes. This is attested by experiments done by both other researchers [18] and our colleagues. For example, MPI\_Alltoall with 1000 integers spent 0.21s on 8 processes and up to 10s on 32 processes testing on ZiQiang3000 cluster at Shanghai Uni-versity, which has 174 computing nodes, two 3.06GHz Intel Xeon CPUs and 2GB memory per node, and Infiniband internet-worked. Its Linpack performance reaches to 1.51 TFLOPS [19].

The complexity estimation for communication time might be expressed as:

$$T_{c2} = O(N_w P^2 + N_w P) < O(2NP^2)$$

$$T_{c3} = O(2N_k P^2) < O(2NP^2)$$

$$T_{c5} = O(P)$$

The memory requirement of communication mainly resides at the buffer for maximum data elements to be sent or received. That is about the double memory amount for storing a spatial complex vector for each wall facet. Thus, memory overhead for communication can be estimated as:

$$M_c = O(12N_w) < O(12N)$$

One note remarkable is that it's better to allocate communication buffers from the heap as global variables rather from the function stack as local variables in order to timesaving on allocation and keeping from stack overflow on runtime.

#### 4. Experimental results and discussions

This section will present some experimental results to demonstrate the validity of the parallel algorithm proposed in this paper.

The first thing to be made sure is that the RCS values obtained by the parallel hybrid algorithm should be consistent with that computed by the serial version. Below just one case of a circular straight cavity CS06 with  $N = 604, N_i = 10, \phi$

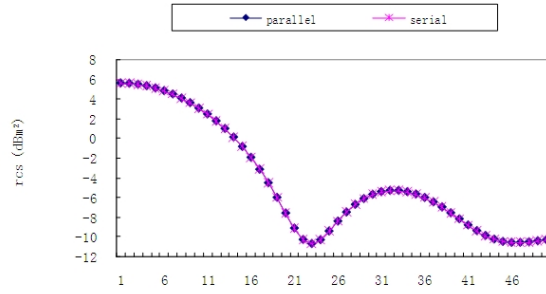


FIGURE 7. Comparison of RCS results for case CS06.

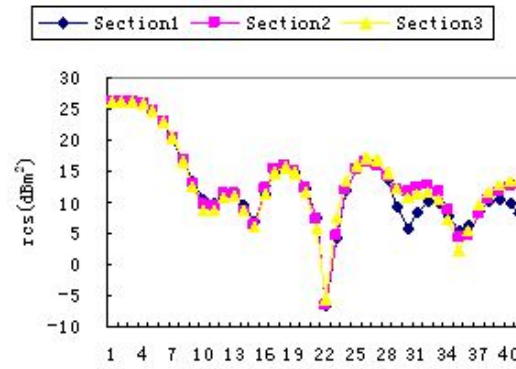


FIGURE 8. Comparison of RCS results for case CF104.

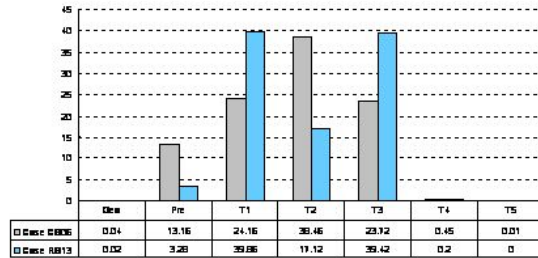


FIGURE 9. Comparison of computing time ratio on each step for case CS06 and RS13.

polarization is presented in Figure 7 to demonstrate the correctness of the parallel algorithm implemented. Figure 8 presents another test case CF104 with  $N = 104444$ ,  $N_i = 10$ ,  $\phi$  polarization to show the consistence of RCS results by dividing the cavity into one, two or three sections.

The parallel solution adopts a hybrid algorithm of serial geometric processing and parallel electromagnetic computing. To verify the reasonableness of this hybridism, an experimental measure on the computing time of each step is given in

Figure 9 . It shows that  $T_{geo}, T_5, T_4$  are revealed to be in the minority. This holds true for all examples tested. And  $T_{geo}$  will weigh even more less when the number of unknowns becomes larger.

Estimate results about memory consumption and distribution efficiency for six cases are given in Table 4 ,where 'CS' denotes circular straight cavity, 'CF' for circular flexural cavity, and 'RS' for rectangle straight cavity. It can be seen that communication induces less than 5% memory overhead. The absolute value is independent of parallel degree. Table 4 also helps to testify that a full replication of geometric data structures (vertexes, edges, area, normal, and topology relations inclusive) on each process is acceptable even when the number of unknowns goes up to four hundred thousand. The distribution efficiency for memory is somewhat variable. It changes with several factors such as the cavity shape, the angle sample number and the parallel degree. A range of distribution efficiency from 60% to 97% is yielded for the cases listed in Table 4.

It is well known that the parallel efficiency  $E_p$  is the key performance measure to be assessed. The efficiency  $E_p$  is measured over 90% for two small scale problems which serial time  $T_1$  can be obtained by experiments, see Figure 10 .Because most test cases go beyond one processor as regard to memory or computing time, the scalability  $\eta$  is instead evaluated as an alternate to the original  $E_p$  The scalability [20][21] in this paper is defined as

$$(13) \quad \eta_J = \frac{IT_I}{JT_J} \times 100\%$$

$T_I$  is the execution time with  $I$  processors and  $T_J$  is the execution time with  $J$

TABLE 4. Estimation of the distribution efficiency for six cases

Case	$M_1(MB)$	$M_{geo}/M_1(\%)$	$M_c/M_p(\%)$	$D_P(\%)$	
				$P = 4$	$P = 8$
$CS06 : N = 648,$ $K = 1$	4.84	7.74	1.90	77.62	60.07
$RS13 : N = 13270,$ $K = 1$	179.11	4.11	1.18	86.68	73.86
$RS27 : N = 27134,$ $K = 1$	474.23	3.17	0.94	89.39	78.53
$CF104 : N = 104444,$ $K = 2$	5651.43	1.02	0.23	96.31	91.90
$RF200 : N = 200880,$ $K = 3$	12740.26	0.84	0.18	96.94	93.23
$CS391 : N = 391840,$ $K = 3$	21930.97	0.96	0.22	96.53	92.35

processors. Figure 11 shows the scalability of three cases RS27, CF104 and RF200 (refer to Table 4 ), where the value of  $I$  in  $\eta_J$  takes the previous neighboring value of  $J$  available in data sheet. The scalability for the three cases reaches nearly above 90%. The results are not bad although the scalability drops a bit as the degree of parallel increases mainly because of the communication overhead being larger.

One disadvantage to the scalability or parallel efficiency in our implementation is that the computation about far-field interaction often introduce load imbalance on processes by the current ADP method. Angle samples are divided into rectangles

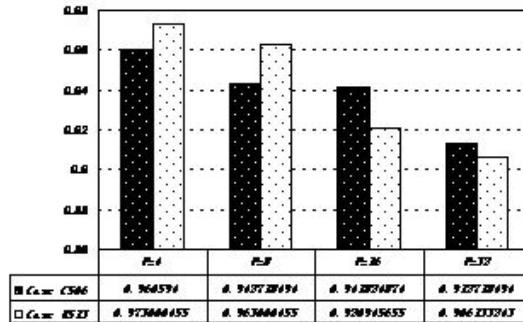


FIGURE 10. Parallel efficiency for case CS06 and RS13.

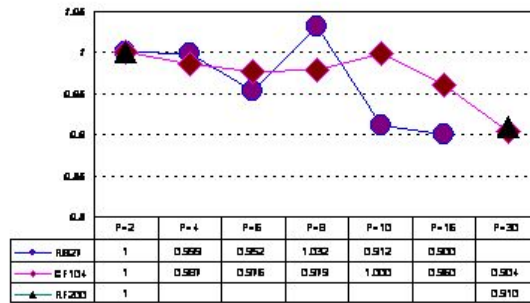


FIGURE 11. Scalability for case RS27, CF104 and RF200.

of not always same number of samples by the implemented partitioning algorithm. Non rectangle partitioning of angle samples has been scheduled as the near-future work.

### 5. Summary

A hybrid algorithm combining IPO, FMM and GRI by Cascading Segmentation technique is adopted as an efficient and accurate way to compute RCS of arbitrary cavities. The RCS problem of cavities is computation intensive and memory intensive. To extend the range of problems that can be solved by the serial version of the hybrid algorithm, a parallel implementation using Message Passing Interface is presented in this paper. The parallel solution tries to distribute computation workload and memory requirement evenly on some distributed memory processes to deal with the embarrassingly scaling of cavity problems.

The parallel algorithm is somewhat hybrid in that it applies a serial approach and a parallel approach to the two phases of RCS analysis respectively. In the phase of geometrical preprocessing, the whole geometry dissected data is provided for each process so that the topology can be constructed independently. This is validated by the relatively small geometrical memory requirements and the extensive involvement of geometric information in next phase. A full replication of geometric data structures cuts down much communication and helps to greatly speed up the

subsequent parallel computation. In the phase of electromagnetic computing, a hybrid parallelization technique is used. The near-field electro-magnetic interaction workload is distributed based on the domain decomposition of wall facets and cover facets, while angle samples based domain decomposition is used to distribute far-field workload.

This parallel algorithm introduces almost no extra computation to that in serial version although certain overhead is introduced in communication time and communication buffer (generally less than 5%). The communication time increases remarkably with the number of processes. In test cases, although several or even tens of seconds might be consumed by communication in one iteration, it is still relatively small and optimal as hundreds or thousands of seconds may be spent by the iterative computation even with a small cavity problem of thousand unknowns. The superposition of electromagnetic measures and permutability of math vector operations helps achieve minimal communication overhead by independent partial computation before the last reduction operation.

The parallel solution can be used to solve any electrically large, deep and arbitrary shaped cavities. Complexity analysis indicates good distribution of computation workload. The distribution of memory requirement is to some extent dependent on the target problem. By leveraging memory, the hybrid parallel solution cuts down much communication overhead and yields very good performance. Experiment results show near-linear scalability and over 90% parallel efficiency. The parallel efficiency may be further improved with better infrastructure network and better algorithm to partition angle samples.

## References

- [1] F.O.Basteiro, J.L.Rodriguez and R.J.Burkholder, An Iterative Physical Optics Approach for Analyzing the Electromagnetic Scattering by large Open-Ended Cavities, *IEEE Transactions on antennas and propagation*, 43(4) :356-361,1995.
- [2] J.L.Rodriguez, F.Oelleiro and A.G. Pino, Iterative Solutions of MFIE for Computing Electromagnetic Scattering of Large Open-Ended Cavities, *IEEE Proc antennas and propagation*, 144(2) :141-144,1997.
- [3] F.O.Basteiro, J.Campos-Nino, J.L.Rodriguez and A.G.Pino, A Segmented Approach for Computing the Electromagnetic Scattering of Large and Deep Cavities, *Progress In Electromagnetic Research, PIER* 19, PIER 19:129-145,1998.
- [4] Ling,H and H.Kim, *On the application of Kirchhoff's approximation to scattering from discontinuities in large waveguide ducts*, Microwave and Optical Technology Letters, 7(4): 168-172,1994 .
- [5] Wei Luo , Zhenping Gao and Huaiwu Zhang , *Fast Calculate the RCS of Electrically Large Cavity by IPO+FMMA Combined with the GRI and Connection Technology*, Journal of Electronics Information Technology, 29(9): 2269-2273,2007.
- [6] E.J.Lu and D.I.Okunbor, *A Massively Parallel Fast Multipole Algorithm in Three Dimensions*, In The Proceedings of Fifth IEEE International Symposium on Parallel and Distributed Processing, 40-48,1996.
- [7] C.C. Lu and W.C. Chew, *Fast Far-field Approximation for Calculating the RCS of Large Objects*, Microwave and Optical Technology Letter, 8(5):238-241,1995.
- [8] Wu Wang, Yangde Feng and Xuebin Chi, *Parallel electromagnetic simulation for electric large target by EMS-FMM*, In the fifth International Conference on Frontier of Computer Science and Technology(FCST) 2010, 36-39,2010.
- [9] Huapeng Zhao, Jun Hu and Zaiping Nie , *Parallelization of MLFMA with composite load partition criteria and asynchronous communication*, Applied Computational Electromagnetics Society Journal, 25(2):167-173,2010.
- [10] S.Velamparambil, W.Chew and J.Song, *On the Parallelization of Dynamic Multilevel Fast Multipole Method on Distributed Memory Computers*, in Innovative Architecture for Future Generation High-Performance Processors and Systems,IEEE Comput. Soc. Press, 3-11,2000.

- [11] Xiaoyan Xue, Xiaoli Zhi, Hailing Guo, Xinqiang Wang and Weili Ni, *Implementation of Parallel Computing for Electromagnetic Scattering by Large Cavities*, IN 2008 China-Japan Joint Microwave Conference, 350-353, 2008.
- [12] Ting Wang, Yue Hu, Yanbao Cui, Weiqin Tong and Xiaoli Zhi, *The load balancing algorithm based on the parallel implementation of IPO and FMM*, In High Performance Computing and Applications - Second International Conference, HPCA 2009, 410-417, 2010.
- [13] Yang M.-L. and Sheng X.-Q., *Parallel high-order FE-BI-MLFMA for scattering by large and deep coated cavities loaded with obstacles*, Journal of Electromagnetic Waves and Applications, 23(13):1813-1823, 2009.
- [14] S. Velamparambil and W.C.Chew, *Analysis and Performance of a Distributed Memory Multilevel Fast Multipole Algorithm*, IEEE Transaction on antennas and propagation., 53(8): 2719-2727, 2005.
- [15] Argonne National Laboratory, <http://www.mcs.anl.org/mpi/mpich/>
- [16] S. Velamparambil, J. Song and W. Chew, *On the Parallelization of Electrodynamics Multilevel Fast Multipole Method on Distributed Memory Computers*, In 1999 International Workshop on Innovative Architecture, 301, 1999.
- [17] S. Velamparambil, W. Chew and J. Song, *10 Million Unknowns: Is It That Big?*, IEEE Antennas and Propagation Magazine, 45(2): 43-58, 2003.
- [18] Y. Weng, J. Fang, Y. Che, Z. Wang, *Performance Analysis of All-to-all on Gigabit Ethernet Cluster (Chinese)*, In proc. National conference of computer network and communication, 69-72, 2009.
- [19] High Performance Computing Center at Shanghai University, <http://www.hpcc.shu.cn>
- [20] V. Kumar and A. Gupta, *Analysis of Scalability of Parallel Algorithms and Architectures*, Journal of Parallel and Distributed Computing, 22(3):379-391, 1994.
- [21] J. Nesheiwat and B.K. Szymanski, *Scalable Performance Analysis for Parallel Scientific Computations, Engineering Simulation*, in Innovative Architecture for Future Generation High-Performance Processors and Systems, 18(2):179-198, 2001.

School of Computer Engineering and Science, Shanghai University, Shanghai, NL 200072, China

*E-mail:* xlzhi@mail.shu.edu.cn